JOURNAL OF CATALYSIS 126, 299–305 (1990)

Catalytic Activity and Si, Al, P Ordering in Microporous Silicoaluminophosphates of the SAPO-5, SAPO-11, and SAPO-37 Type

JOHAN A. MARTENS, PIET J. GROBET, AND PETER A. JACOBS

Laboratorium voor Oppervlaktechemie, Katholieke Universiteit Leuven, Kardinaal Mercierlaan 92, B-3030 Heverlee, Belgium

Received February 16, 1990; revised June 18, 1990

The catalytic activity in the conversion of decane on SAPO-5, SAPO-11, and SAPO-37 samples with Si *T*-atom fractions ranging from 1 to 42% were determined. The relationship of catalytic activity with compositional parameters is discussed. Due to the nonuniform distribution of silicon, aluminium, and phosphorus over individual crystals, the overall chemical composition of a SAPO-*n* sample is unable to rationalize its catalytic activity. In order to explain the catalytic activity of SAPO-5, SAPO-11, or SAPO-37 materials, the contributions of aluminosilicate (SA) and silicoaluminophosphate (SAPO) crystal domains have been determined using ^{29}Si MAS NMR. Acid sites located in the SA and SAPO domains and at their interphases contribute to the catalytic activity. The contribution of the different types of acid sites to the catalytic activity is strongly dependent on the SAPO-*n* structure type.

INTRODUCTION

Microporous crystalline silicoaluminophosphate molecular sieves have been patented by Lok *et al.* (*1*) and are denoted as SAPO-*n*, in which *n* stands for the structure type. SAPO-5 has the AFI topology (*2*) and consists of nonintersecting 12-membered ring (12-MR) pores with a free diameter of 0.73 nm (*2*). SAPO-11 crystals have the AEL structure-type and are permeated by nonintersecting elliptic 10-MR pores with minimum and maximum diameter of 0.39 and 0.63 nm, respectively (*2*). SAPO-37 has the FAU topology and is isostructural with zeolite Y (*2*). The void volume of the FAU structure consists of so-called supercages, with a free diameter of ca. 1.3 nm. Its four apertures consist of regular 12-MRs with a diameter of 0.74 nm (*2*).

There seem to exist some general rules concerning the nature of the nearest *T*-atom neighbors (NN) of Si, Al, and P in SAPO-*n* molecular sieve zeolites (*3*). These elements appear as Si(*n*Si, 4-*n*Al), P(4Al), Al(*m*Si, 4-*m*P) environments, respectively, with $1 < m,n < 4$. This does not preclude that the crystal chemistry of SAPO-5, SAPO-11, and SAPO-37 materials is extremely complex. Synthesis methods have been developed to generate samples of SAPO-5, SAPO-11, and SAPO-37 in which the *T*-atom composition is not uniform throughout the individual crystals (*4–6*). These crystals contain aluminosilicate (SA) domains, where the silicon is concentrated, next to silicoaluminophosphate (SAPO) domains, where all the phosphorus is located (*4–6*). The *T*-atom compositions of the SA and SAPO domains can be determined with ^{29}Si MAS NMR (*4–6*). In principle, Brønsted acid sites can be present in the SA parts, in the SAPO parts, and at the boundaries between these different domains (*4–6*).

SAPO-*n* materials in the protonic form often show mild acidity, in contrast to aluminosilicate zeolites which are usually stronger Brønsted acids (*7*). According to recent patents and publications, several SAPO-*n* materials have potential catalytic applications in petroleum refining and petrochemical conversion processes (*8*).

0021-9517/90 $3.00

The catalytic activity of aluminosilicate zeolites is related to the Si, Al ordering (*9*). In the present work an attempt is made to rationalize the catalytic activity of SAPO-*n* materials based on their Si, Al, P ordering. The bifunctional conversion of decane was selected for determining the catalytic activities. Indeed, bifunctional catalysis with long-chain *n*-alkanes such as decane offers the advantage that catalytic activities can be measured under nondeactivating conditions (*10*). Bifunctional catalysts contain a noble metal dispersed on an acidic support. According to the classical bifunctional reaction mechanism, the activity of a bifunctional catalyst is determined by its Brønsted acidity (*11, 12*).

EXPERIMENTAL

The SAPO-5, SAPO-11, and SAPO-37 samples are denoted as S-5/*n*, S-11/*n*, and S-37/*n*, respectively, in which *n* stands for the sample number. The synthesis of the S-5 and S-11 samples using cyclohexylamine and dipropylamine, respectively, was described previously (Refs. (*4, 5*)). They were calcined at a temperature of 823 K to remove the template. SAPO-37 materials were synthesized with both tetramethylammonium (TMA) and tetrapropylammonium (TPA) hydroxide as template. The method is described in detail in Ref. (*6*). The molar composition of the gels used for the synthesis of S-37 samples is given in Table 1. In the gel used for the synthesis of the S-37/2 and S-37/3 samples, the Si content was increased and the P content decreased with respect to that used for sample S-37/1, while keeping the water, TPA, TMA, and aluminium content constant. S-37/4 was obtained from the same gel as S-37/3 by prolonging the crystallization time from 24 to 48 h.

TABLE 1

Molar Oxide Ratios per Mol of Al_2O_3 in the Synthesis of SAPO-37

	TMA_2O	TPA_2O	SiO_2	P_2O_5	H_2O
S-37/1	0.026	0.992	0.435	1.043	49.4
S-37/2	0.026	0.992	0.636	0.932	49.2
S-37/3	0.026	0.992	0.864	0.818	49.2
S-37/4	0.026	0.992	0.864	0.818	49.2

TABLE 2

T-Atom Composition $(Si_xAl_yP_z)O_2$, Template Volume[a] and Micropore Volume[b] of S-5, S-11, and S-37 Samples

Sample	Si x	Al y	P z	Template volume ($cm^3\ g^{-1}$)	Micropore volume ($cm^3\ g^{-1}$)
S-5/1	0.01	0.50	0.49	0.15	ND[c]
S-5/2	0.15	0.44	0.41	0.11	0.10
S-5/3	0.19	0.43	0.38	0.15	0.11
S-5/4	0.28	0.39	0.33	0.14	0.09
S-11/1	0.04	0.52	0.44	0.16	0.02
S-11/2	0.21	0.43	0.36	0.11	ND
S-11/3	0.39	0.33	0.28	0.14	ND
S-11/4	0.42	0.31	0.27	0.11	0.05
S-37/1	0.16	0.49	0.36	0.44	ND
S-37/2	0.21	0.46	0.33	0.35	ND
S-37/3	0.23	0.43	0.34	0.34	ND
S-37/4	0.29	ND	ND	0.31	ND

[a] Using the liquid phase density of adsorbed template.
[b] Volume of adsorbed N_2 at $P/P_0 = 0.3$.
[c] ND = not determined.

Zeolite Y was a NaY sample with Si/Al ratio of 2.5, exchanged for 90% with NH_4Cl.

The chemical composition of the samples is given in Table 2. The volumes occupied by the template in the as-synthesized samples, also given in Table 2, were calculated using its liquid phase density. The micropore volumes of calcined samples were determined as the total volumes of adsorbed nitrogen at $P/P_0 = 0.3$. The *T*-atom composition of the SA and SAPO domains and their contribution to the crystals, was determined by ^{29}Si MAS NMR (*4–6*), and is given in Table 3.

The S-5/*n* and S-11/*n* samples were impregnated with an aqueous solution of Pt $(NH_3)_4Cl_2$ and dried subsequently at 325 K. Oxygen calcination and hydrogen reduction was performed at 673 K *in situ* in the reactor. The as-synthesized S-37/*n* samples were

TABLE 3

Contribution to the Total Chemical Composition of SA and SAPO Domains[a] and Their Respective *T*-Atom Composition

Sample	Contribution of domains		*T*-Atom composition				
	SAPO (%)	SA (%)	SA domains		SAPO domains		
			Si (%)	Al (%)	Si (%)	Al (%)	P (%)
S-5/1	100	0	—	—	1	50	49
S-5/2	90	10	100	0	6	50	44
S-5/3	86	14	100	0	6	50	44
S-5/4	75	25	94	6	6	50	44
S-11/1	94	6	66	33	0	50	50
S-11/2	72	28	66	33	0	50	50
S-11/3	56	44	87	13	0	50	50
S-11/4	54	46	90	10	0	50	50
S-37/1	92	8	60	40	12.5	50	37.5
S-37/2	82	18	65	35	12.5	50	37.5
S-37/3	79	21	66	34	12.5	50	37.5
S-37/4	69	31	69	31	12.5	50	37.5
Y	0	100	71	29	—	—	—

[a] Determined by deconvolution of the ^{29}Si MAS NMR spectra, as described in earlier work (Refs. (*4–6*)).

first exchanged with NH_4Cl. Accordingly, the TPA content was reduced with ca. 50%, while the TMA content was unaffected. Subsequently, they were exchanged with $Pt(NH_3)_4Cl_2$. It was verified that the crystallinity was maintained after oxygen calcination and hydrogen reduction at 673 K. Zeolite Y was loaded with platinum in the same way as the SAPO-37 samples. The Pt loading of all catalysts was 0.5% by weight.

Decane isomerization and hydrocracking was performed in a homemade fully automated continuous flow microreactor. Product analysis was done with an HP 5890 GC, equipped with a capillary CPSil-5 column from Chrompack, with an internal diameter of 0.31 mm and a length of 50 m. The zeolite powders were compressed into flakes, which were crushed into particles with a diameter between 0.25 and 0.50 mm. A bed containing 100 or 200 mg of catalyst pellets was fixed in a reactor tube of 1-cm width. At the inlet of the reactor, the partial pressure of hydrogen and decane was 0.35 MPa and 3.5 kPa, respectively. The space time, W/F_0 (kg s mmol^{-1}) was varied. W is the catalyst weight and F_0 the molar flow rate of decane at the bed entrance.

The ^{29}Si MAS NMR experiments were run using a Bruker 400 MSL spectrometer working at 79.5 MHz, with a pulse length of 3 μs, a repetition time of 3 s, and a spinning rate of 3 kHz. The number of scans was at least 10,000. The chemical shift reference was tetramethylsilane (TMS). The different lines in the ^{29}Si MAS NMR spectra were deconvoluted using the Bruker GLINFIT program (*13*) using the Gaussian line shape.

RESULTS AND DISCUSSION

SA and SAPO Domains in SAPO-5, SAPO-11, and SAPO-37 Crystals

A schematic representation of the *T*-atom ordering in a SAPO-*n* crystal with SA and SAPO domains is given in Fig. 1. The SAPO part can be considered to be derived from an $AlPO_4$ framework, with a strict alternation of Al and P atoms, in which part of the P atoms are replaced with Si. Thus each Si atom in the SAPO domains appears in Si(4Al) environment and generates a SAPO-type Brønsted acid site. All nearest neighbors (NN) of Si are Al atoms. In the SAPO part of the crystal, all second nearest neighbors (SNNs) of Si are P-atoms.

The SA part of the crystal does not contain phosphorus. Each Al atom introduced a net negative lattice charge and one SA-type Brønsted acid site. Si and Al appear as NNs

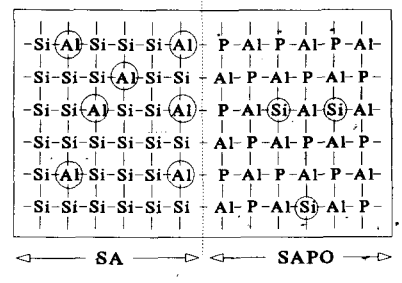

FIG. 1. Schematic representation of Si, Al, and P environments in the SA and SAPO domains of SAPO-*n* crystals. The encircled elements introduce Brønsted acid sites.

and SNNs of Si. On the SA side of the interphases between the SA and SAPO domains, Si environments are present, characterized by having Si, Al, and P as possible SNNs. In previous work it was suggested that such interphase-type Brønsted acid sites in SAPO-37 may be important sites for acid catalysis (*6*).

For S-5 and S-11-type samples, the proportions of SA and SAPO domains and their compositions can be determined by ^{29}Si MAS NMR, which allows one to discriminate between Si atoms belonging to the SA and to the SAPO domains (*4, 5*). As an illustration, Fig. 2 shows the experimental and deconvoluted ^{29}Si MAS NMR spectra of some S-5 and S-11 samples. The signal at −92 ppm represents Si(4Al) in SAPO environment. The −112 ppm line is assigned to Si(4Si) in SA domains. The amount of SAPO-type aluminium is considered to be equal to the sum of SAPO-type silicon and phosphorus. The remaining aluminium should be sited in the SA domains. A hypothetical example of the distribution of the *T*-atoms between both domains is schematically shown in Fig. 1. Some of the Al atoms at the interphases between SA and SAPO domains are considered to belong to the SA domain. Such Al atoms occur in Al(3Si1P) configuration and should generate the interphase-type Brønsted acidity.

The contributions of SA and SAPO domains to the samples and their *T*-atom compositions are listed in Table 3. In the S-5 sample series, the contribution of the SA domains increases from 0 to 25% with increasing overall Si content. The Si content of the SAPO domains is restricted to some 6% (Table 3).

The silicon content of the SAPO domains of the S-11 sample series is very low (Table 3). Figure 2 illustrates that signals due to Si(4Al) are absent in the ^{29}Si MAS NMR spectrum of S-11/2. The Al content of the SA domains of the SAPO-11 samples with the lowest amount of SA domains (S-11/1 and S-11/2) is 33% (Table 3). When the contribution of the SA domains is increasing

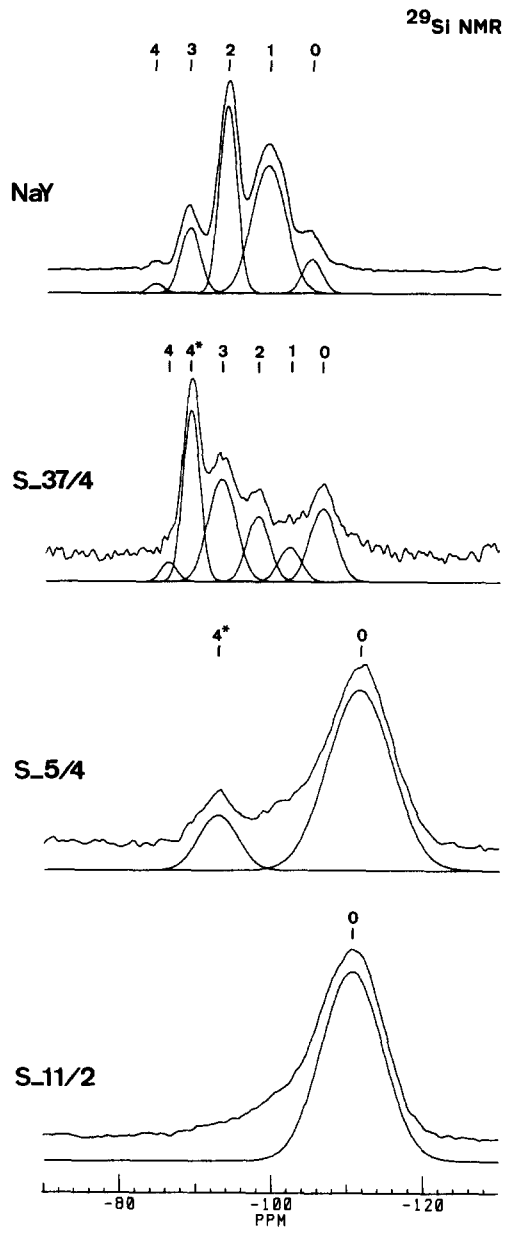

FIG. 2. Experimental and deconvoluted ^{29}Si MAS NMR spectra of NaY, S-37/4, S-5/4, and S-11/2 samples. The number of NN Al atoms are indicated on the spectra. Coordinations in SAPO domains are indicated with an asterisk.

(samples S-11/3 and S-11/4), the Al content of the SA domains remains typically between 10 and 13% (Table 3).

Experimental and deconvoluted ^{29}Si MAS NMR spectra of S-37/4 are shown in Fig. 2.

For comparison, the ^{29}Si MAS NMR spectrum of zeolite NaY is added. The SAPO-type silicon appears at a chemical shift of -89.4 ppm. The other Si signals at -86.4, -93.4, -98.2, -102.3, and -106.7 ppm represent SA-type silicon in Si(4Al), Si(3Al1Si), Si(2Al2Si), Si(1Al3Si), and Si(4Si) environments, respectively. The SAPO domains of the different SAPO-37 samples have the same *T*-atom composition and contain 12.5% Si (*6*). If for the calculation of the composition of the SA domains in S-37/4, the same approach is used as for the S-5 and S-11 samples, an aluminum content of 33% is found (Table 3). The composition of the SA and SAPO domains in the other SAPO-37 samples was determined in the same way (Table 3). The SA domains in the SAPO-37 samples become more siliceous when such domains are more abundantly present (Table 3).

Catalytic Activity of SAPO-5 and SAPO-11

The degree of conversion of decane over the S-5 and S-11 catalysts at a reaction temperature of 543 K has been plotted in Figs. 3 and 4 versus its space time. The activity sequence for the SAPO-5 catalysts series is

$$\text{S-5/1} \ll \text{S-5/4} < \text{S-5/3} < \text{S-5/2}$$

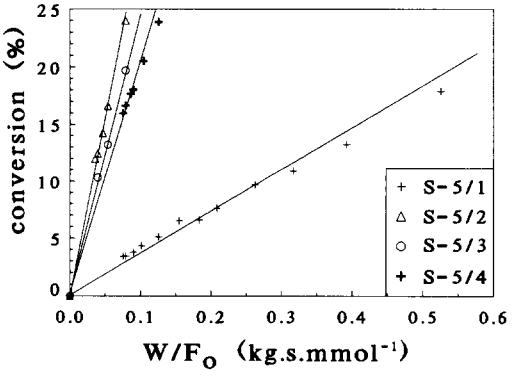

FIG. 3. Degree of conversion of decane over S-5 samples at a reaction temperature of 543 K against space time, W/F_0.

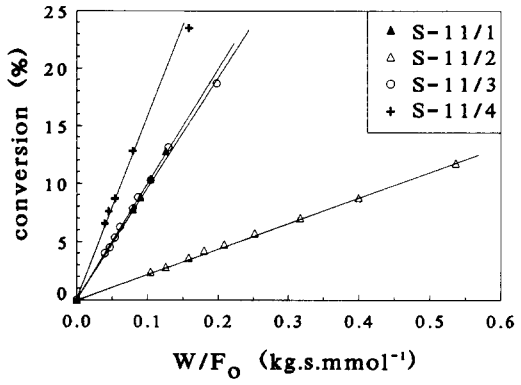

FIG. 4. Degree of conversion of decane over S-11 samples at a reaction temperature of 543 K against space time, W/F_0.

while for the SAPO-11 series it is

$$\text{S-11/2} < \text{S-11/3} = \text{S-11/1} < \text{S-11/4}.$$

Initial reaction rates for decane conversion were derived from the slopes of Fig. 3. When these rates are plotted against the Si content of the SAPO-5 samples (Fig. 5A), a maximum activity is observed for a Si T-atom fraction of 0.15. SA domains are absent in S-5/1 (Table 3). In S-5/2, the SA domains do not contain aluminium (Table 3) and, consequently, do not contain Brønsted acid sites. S-5/2 contains six times more SAPO-type acid sites compared to sample

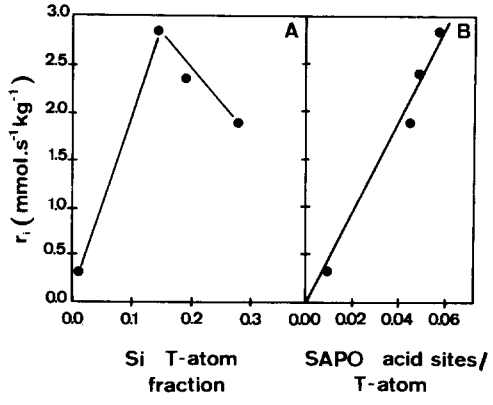

FIG. 5. Initial rates of decane conversion, r_i, at 543 K against Si *T*-atom fraction and number of SAPO-type acid sites/*T*-atom of S-5 samples.

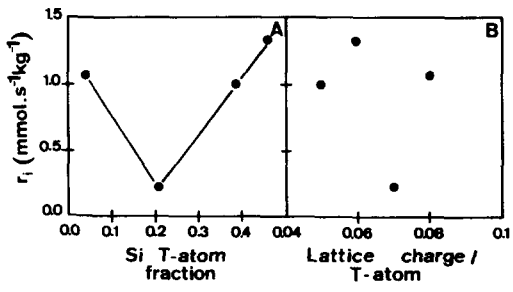

FIG. 6. Initial rate of decane conversion, r_i, at 543 K against Si *T*-atom fraction and overall lattice charge/*T*-atom of S-11 samples.

S-5/1 (Table 3). The latter zeolite is ca. seven times more active (Fig. 3). The turnover number of the SAPO-type acid sites in SAPO-5, evaluated from the initial rates of decane conversion over S-5/1 and S-5/2, is $3.0 \pm 0.5\ 10^{-3}\ s^{-1}$. Furthermore, for the S-5 series of samples, the initial rate of decane conversion is proportional to the amount of SAPO-type acid sites in the catalyst (Fig. 5B). The proportionality between catalytic activity and SAPO-type acidity suggests that the SA domains and the SA–SAPO interphases do not contribute to the catalytic activity. This is consistent with the absence of aluminium in the SA domains (Table 3).

Figure 6 shows the initial rate of decane conversion versus the Si *T*-atom fraction and versus the average lattice charge per *T*-atom of SAPO-11 catalysts. In contrast to the SAPO-5 series, a minimum activity is observed for the SAPO-11 sample with intermediate Si content (Fig. 6A). Figure 6B shows that the overall lattice charge, calculated from the chemical compositions of Table 3, does not provide a way to rationalize the catalytic activity. The S-11 samples do not contain SAPO-type acid sites, since the SAPO domains do not contain silicon (Table 3). Nevertheless, the initial rate of decane conversion over the S-11 catalysts is of the same order of magnitude as over the S-5 catalysts (Fig. 5). In the S-11 samples the activity should, therefore, be related to the presence of SA–SAPO interphase-type and SA-type of acid sites.

Catalytic Activity of SAPO-37

The conversion curves of decane over the S-37/1-4 samples and over zeolite Y at a reaction temperature of 503 K are shown in Fig. 7. The S-37 samples are generally more active than the S-5/*n* and S-11/*n* samples, which were tested at a reaction temperature of 543 K (Fig. 3). The activity sequence is

$$\text{S-37/2} < \text{S-37/1} < \text{S-37/3} < \text{S-37/4} = \text{HY}.$$

The SAPO domains of all the S-37 samples have the same composition (Table 3). The increased activity of S-37/3 and S-37/4 with respect to S-37/1 and S-37/2 should reflect a contribution of the SA domains and SA–SAPO interphases of these samples. It is generally accepted that the strongest acid sites in an aluminosilicate are those associated with Al atoms with only Si in NN and SNN positions (*14*). The Si(*n*Al) distribution of the SA domains in the different SAPO-37 samples and in zeolite Y are given in Table 4. Table 4 shows that the Si(*n*Al) distributions of the S-37 samples exhibit a minimum at Si(1Al). Therefore, the number of this type of acid sites should be very small, in contrast to zeolite Y where the Si(1Al) con-

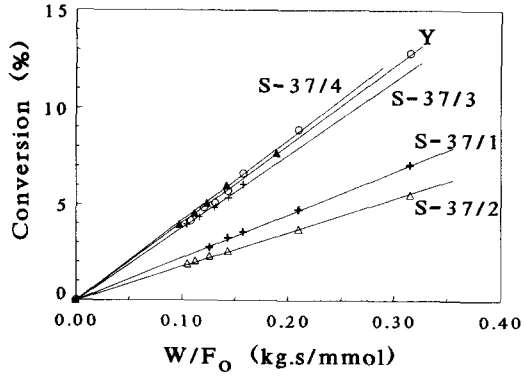

FIG. 7. Conversion of decane versus space time, W/F_0, over S-37 and zeolite Y samples at a reaction temperature of 503 K.

TABLE 4

Distribution of Si(nAl) Coordinations in the SA Domains of SAPO-37 and in Zeolite Y

	Si(4Al) (%)	Si(3Al) (%)	Si(2Al) (%)	Si(1Al) (%)	Si(0Al) (%)
S-37(1)	26	48	10	0	16
S-37(2)	9	43	21	9	18
S-37(3)	12	41	16	7	24
S-37(4)	4	39	19	11	26
Y	1	12	39	41	8

figuration is most abundant. The observation that the catalytic activity of S-37/4 is comparable to that of zeolite Y can only be explained if at the boundary between the SA and SAPO domains, acid sites with very high turnover numbers are present.

CONCLUSIONS

The catalytic activity of SAPO-5, SAPO-11, and SAPO-37 samples cannot be rationalized by the concepts of overall lattice charge or overall Si content. It is essential to determine the contribution of SA and SAPO domains and their T-atom compositions. This can conveniently be done by ^{29}Si MAS NMR and chemical analysis. The catalytic activity of SAPO-5 crystals is located in the SAPO domains. The SA domains are siliceous and do not contain catalytically active Brønsted acid sites. In SAPO-11 crystals, the activity seems to be due to SA–SAPO interphase-type and SA-type acidity. The active sites of SAPO-37 catalysts are located in the SAPO domains, in the SA domains, and at the domain boundaries. The latter type of active sites should exhibit extraordinarily large turnover numbers.

ACKNOWLEDGMENTS

J.A.M. and P.J.G. acknowledge the Belgian National Fund for Scientific Research for Research Positions. The authors are grateful to M. Mertens for the preparation of the SAPO-5 and SAPO-11 samples. This research has been sponsored by the Belgian Government in the frame of a Concerted Action on Catalysis.

REFERENCES

1. Lok, B. M., Messina, C. A., Patton, R. L., Gajek, R. T., Cannan, T. R. and Flanigen, E. M., U.S. Patent 4,440,871 (1984).
2. Meier, W. M., and Olson, D. H., "Atlas of Zeolite Structure Types," 2nd ed. Butterworths, London, 1987.
3. Flanigen, E. M., Patton, R. L., and Wilson, S. T., *Stud. Surf. Sci. Catal.* **37,** 13 (1988).
4. Martens, J. A., Mertens, M., Grobet, P. J., and Jacobs, P. A., *Stud. Surf. Sci. Catal.* **37,** 97 (1988).
5. Mertens, M., Martens, J. A., Grobet, P. J., and Jacobs, P. A., NATO ASI Ser., submitted for publication.
6. Martens, J. A., Janssens, C., Grobet, P. J., Beyer, H. K., and Jacobs, P. A., *Stud. Surf. Sci. Catal.* **49,** 215 (1989).
7. Lok, B. M., Messina, C. A., Patton, R. L., Gajek, R. T., Cannan, T. R., and Flanigen, E. M., *J. Amer. Chem. Soc.* **106,** 6092 (1984).
8. Rabo, J. A., Pellet, R. J., Coughlin, P. K., Shamshoum, E. S., *Stud. Surf. Sci. Catal.* **46,** 1 (1989).
9. Barthomeuf, D., *in* "Zeolites: Science and Technology" (F. R. Ribeiro, A. E. Rodrigues, L. D. Rollmann, and C. Naccache, Eds.), NATO ASI Ser. E, No. 80, p. 317. Nijhoff, The Hague, Boston/Lancaster, 1984.
10. Martens, J. A., Tielen, M., Jacobs, P. A., and Weitkamp, J., *Zeolites* **4,** 98 (1984).
11. Eley, D. D., Selwood, P. W., and Weisz, P. B., Eds., "Advances in Catalysis," Vol. 13, p. 137. Academic Press, New York, 1962.
12. Coonradt, M. L., and Garwood, W. E., *Ind. Eng. Chem. Prod. Res. Dev.* **3,** 38 (1964).
13. Bruker ABACUS Catalog No. ABA078.
14. Wachter, W. A., *in* "Proc. 6th International Zeolite Conference" (Olson, D. and Bisio, A., Eds.), p. 141. Butterworths, Guildford, UK, 1984.